Document made available under the Patent Cooperation Treaty (PCT)

International application number: PCT/US05/009763

International filing date: 24 March 2005 (24.03.2005)

Document type: Certified copy of priority document

Document details: Country/Office: US
                    Number: 60/555,759
                    Filing date: 24 March 2004 (24.03.2004)

Date of receipt at the International Bureau: 25 April 2005 (25.04.2005)

Remark: Priority document submitted or transmitted to the International Bureau in
          compliance with Rule 17.1(a) or (b)

1309285

THE UNITED STATES OF AMERICA

TO ALL TO WHOM THESE PRESENTS SHALL COME:

UNITED STATES DEPARTMENT OF COMMERCE

United States Patent and Trademark Office

April 18, 2005

THIS IS TO CERTIFY THAT ANNEXED HERETO IS A TRUE COPY FROM THE RECORDS OF THE UNITED STATES PATENT AND TRADEMARK OFFICE OF THOSE PAPERS OF THE BELOW IDENTIFIED PATENT APPLICATION THAT MET THE REQUIREMENTS TO BE GRANTED A FILING DATE.

       APPLICATION NUMBER: *60/555,759*
       FILING DATE: *March 24, 2004*
       RELATED PCT APPLICATION NUMBER: *PCT/US05/09763*

Certified by

Under Secretary of Commerce
for Intellectual Property
and Director of the United States
Patent and Trademark Office

PROVISIONAL APPLICATION FOR PATENT COVER SHEET
This is a request for filing a PROVISIONAL APPLICATION FOR PATENT under 37 CFR 1.53(c).

Express Mail Label No. _ER 8586 25917 US_

INVENTOR(S)

Given Name (first and middle [if any])	Family Name or Surname	Residence (City and either State or Foreign Country)
JAGDISH	NARAYAN	RALEIGH, NORTH CAROLINA

Additional inventors are being named on the _____ separately numbered sheets attached hereto

TITLE OF THE INVENTION (500 characters max)

Direct all correspondence to: **CORRESPONDENCE ADDRESS**

☐ Customer Number:

OR

☒ Firm or Individual Name	Jagdish Narayan, Ph. D.
Address	4917 Springwood Drive
Address	

City	Raleigh	State	NC	Zip	27613-1034
Country		Telephone (919)	515-7874	Fax	(919) 515-7642

ENCLOSED APPLICATION PARTS (check all that apply)

☒ Specification *Number of Pages* __17__   ☐ CD(s), Number _____

☒ Drawing(s) *Number of Sheets* __11__   ☐ Other (specify) _____

☐ Application Data Sheet. See 37 CFR 1.76

METHOD OF PAYMENT OF FILING FEES FOR THIS PROVISIONAL APPLICATION FOR PATENT

☒ Applicant claims small entity status. See 37 CFR 1.27.

☐ A check or money order is enclosed to cover the filing fees.

☐ The Director is herby authorized to charge filing
fees or credit any overpayment to Deposit Account Number: _____

☒ Payment by credit card. Form PTO-2038 is attached.

FILING FEE
Amount ($)

$75.00

The invention was made by an agency of the United States Government or under a contract with an agency of the United States Government.

☐ No.

☐ Yes, the name of the U.S. Government agency and the Government contract number are: _____

, [Page 1 of 2]

Respectfully submitted,

SIGNATURE _____

TYPED or PRINTED NAME JAGDISH NARAYAN

TELEPHONE (919) 515-7874 (Daytime)

Date March 24, 2004

REGISTRATION NO. _____
(if appropriate)
Docket Number: _____

USE ONLY FOR FILING A PROVISIONAL APPLICATION FOR PATENT

Methods of Forming Alpha and Beta Tantalum Films with Controlled and New Microstuctures

Summary of the Invention

This invention relates to formation of Alpha tantalum (α –Ta) films with microstructures ranging from amorphous to nanocrystalline to polycrystalline to single crystal on silicon (Si) substrates with and without buffer layers. Thin films of Alpha tantalum (α-Ta) with grain size ranging from nanosize to single crystal and amorphous tantalum (a-Ta) were fabricated by non-equilibrium pulsed laser deposition techniques, and compared their electrical properties and diffusion characteristics with properties of Beta tantalum (β-Ta) films produced by magnetron sputtering. Single-crystal α-Ta films are formed on silicon (Si) substrates with and without buffer layers by domain matching epitaxy (as described in US Patent 5,406,123 by Jagdish Narayan) where integral multiples of lattice planes match across the film-substrate interface. The buffer layers such as titanium nitride (TiN) and tantalum nitride(TaN) are used to provide template for epitaxial growth of α –Ta. Microstructure and atomic structure of these films were studied by X-ray diffraction and high-resolution electron microscopy, while elemental analysis was performed using electron energy loss spectroscopy and X-ray dispersive analysis. The resistivity measurements in the temperature range (10-300K) showed room-temperature values to be 15-30μ Ω-cm for α-Ta, 180-200μ Ω-cm for β-Ta and 250-275μ Ω-cm for a-Ta. The temperature coefficient of resistivity (TCR) for α-Ta and β-Ta were found to be positive with characteristic metallic behavior, while TCR for a-Ta was negative characteristic of high-resistivity disordered metals. We discuss the mechanism

1 *Narayan*

of formation of a-Ta and show that it is stable in the temperature range 650-700^{0}C. Electron energy-loss spectroscopy (EELS) and Rutherford backscattering measurements showed oxygen content in a-Ta films to be less than 0.1%. The EELS and secondary ion mass spectroscopy (SIMS), scanning transmission electron microscope Z-contrast (STEM-Z) imaging and electron energy-loss spectroscopy (EELS) studies show that, after 650°C annealing for 1 hr, a- Ta and single-crystal α-Ta films have less than 10nm Cu diffusion distance while polycrystalline Ta films have substantial Cu diffusion specifically along grain boundaries. Thus, a-Ta and single-crystal α-Ta provide a far superior diffusion barrier for Cu metallization compared to polycrystalline α-Ta and β-Ta films containing grain boundaries. Thus, superior diffusion properties of a-Ta and single-crystal α-Ta, when combined with low-resistivity epitaxial layers of α-Ta, provide an optimum solution for copper metallization in next-generation silicon microelectronic devices.

Background of the Invention

Copper metal (Cu) has attracted considerable attention as an interconnect layer in silicon microelectronic devices because of its low resistivity (1.67μΩ-cm for bulk) and its high resistance against electromigration and stress migration [1,2]. However, the high diffusivity (D ≈ 10^{-8} cm^2/s) of Cu into Silicon makes it a fatal impurity, which reduces the minority carrier lifetime in silicon microelectronic devices [2]. Therefore, a thin diffusion barrier preventing Cu diffusion into silicon is required to integrate Cu as an interconnect

layer. Ta is one of the most promising diffusion barrier materials for Cu metallization due to its relatively high melting temperature (3287K) and high activation energy for lattice diffusion around 4.8eV in bulk Ta. In addition, Ta is thermodynamically stable with respect to Cu as it is almost completely immiscible up to its melting point and does not react to produce any compounds [3,4]. The reaction between Si and Ta requires temperatures as high as 650°C [5], rendering Si/Ta interface reasonably stable. Ta films also form a stable oxide (Ta_2O_5) that provides a protective layer for Cu diffusion and improves adhesion to SiO_2 and protects the underlying Cu from oxidation until a Ta layer has been completely transformed into Ta_2O_5 [6].

The microstructure of thin films plays an important role in governing the properties such as diffusion behavior and electrical conductivity. The electrical resistivity of α-Ta is expected to be an order of magnitude lower than that of β-Ta (180-200μ Ω-cm). The resistivity of single-crystal α-Ta (which has not been produced before) is expected to be even lower due to lack of grain-boundary scattering. Single-crystal as well as amorphous barrier layers are expected to be more robust diffusion barriers, as they lack grain boundaries which act as short circuit diffusion paths, compared with polycrystalline layers. The grain boundaries provide short circuit or rapid diffusion paths because the activation energy along the grain boundaries is around 2.4 eV (half of that of the bulk lattice diffusion) or less depending upon the grain boundary structure. While single crystal α-Ta layers remain stable with temperature, amorphous films are unstable against recrystallization at high temperatures. To prevent the recrystallization at high temperatures, studies have been done to dope the Ta films with dopants like CeO_2 to achieve amorphous Ta films and were found to be stable up to 800°C but have shown a

3 Narayan

considerable increase in the resistivity [7]. Also, low doping with N and O produced nanocrystalline Ta films as diffusion barriers stable up to 600°C [8-9]. To meet the requirement of lower RC delay in the integrated circuits for future generation devices there is a considerable demand of low resistivity barrier layers [2]. So it is important to study how the diffusion barrier and electrical properties vary as a function of microstructure of Ta films, ranging from amorphous to nanocrystal to polycrystal to single-crysatal. In this study, various microstructures of Ta films were obtained and the effect of the microstructure on the diffusion behavior of Cu and on electrical properties were analyzed. Scanning transmission electron microscopy-Z (STEM Z) contrast imaging which gives different contrast of the element due to its different atomic number (Z^2 dependence) and electron energy-loss spectroscopy (EELS), which allows compositional analysis by detecting the characteristic energy-loss of the electron of the particular element, provide powerful tools to determine the diffusion profile of Cu with a great precision (0.16nm). These results are compared with overall SIMS profiles where resolution is of the order of 10nm. Thus, using HRTEM, STEM-Z contrast imaging and EELS, atomic structure imaging and compositional analysis were obtained on α-Ta films with microstructure ranging from amorphous to single crystal, and the results compared with large-area SIMS studies. We discuss the effectiveness of amorphous and single-crystal films as Cu diffusion barrier layers for next-generation silicon microelectronic devices.

Detailed Description

The present invention will now be described more fully including the experimental procedure hereinafter with reference to accompanying drawings, in which embodiments

of the invention are shown. However, this invention should not be construed as limited to the embodiments set forth herein. Rather, these embodiments are provided so that disclosure will be thorough and complete, and will convey fully the scope of the invention to those skilled in the art. The present invention is summarized in Figure 1 in which embodiments of the invention are shown. In the drawings, relative sizes of thin films may be exaggerated for clarity. Moreover, each embodiment described and illustrated herein includes its complementary conductivity type embodiment as well. Figures 1(a) and 1(b) are cross-sectional views of microelectronic structures that may be fabricated according to some embodiments of the present invention. As shown in Figure 1(a), silicon substrate **1100**, for example a (100) silicon substrate, is provided. Techniques for fabricating silicon substrates are well known to those skilled in the art and need not be described further herein. Also shown in Figure **1100**, a Ta thin film with amorphous, nanocrystalline, polycrystalline and single crystal structures of α (alpha) and β (beta) phases, is formed directly on the silicon substrate **1100**. In some embodiments, domain epitaxy (as described, for example, in U. S. Patent 5,406,123) may be used to single crystal Ta films directly on the silicon substrate **1100**. As shown in Figure 1(b), in some embodiments, a buffer layer **1120** is formed prior to growth of Ta **1110**. These buffer layers (for example, TiN or TaN) may be grown in the form of single crystal which facilitate the formation of single crystal Ta films

For some embodiments, Si (100) substrates were cleaned to remove the native oxide layer around 1.5nm thick using HF solution, and create hydrogen-terminated (100) Si

surfaces . Uniform films of Ta were deposited on Si (100) by Laser MBE (molecular beam epitaxy) for nano, polycrystal and single-crystal α-Ta films, pulsed laser deposition (PLD) for a-Ta, and by dc Magnetron Sputtering (MS) β-Ta. For diffusion studies, in-situ deposition of uniform Cu layer on the Ta/Si(100) substrates was carried out using PLD. For PLD, the films were deposited inside a stainless-steel vacuum chamber evacuated by a turbo molecular pump to a base pressure of 1×10^{-7} Torr, where a KrF excimer laser (λ=248 nm, $\tau \sim$ 25ns) was used for the ablation of Ta and Cu targets. The hot pressed Ta and high purity Cu targets, mounted on a rotating target holder, were ablated at an energy density of 3.0-3.5 J/cm^2. Ta and Cu films were deposited at a laser repetition rate of 5-10Hz for 20 and 10 minutes achieving thickness of 50nm and 20nm, respectively. For Laser-MBE, an ultra-high-vaccum chamber equipped with high-power KrF laser was used for forming layers, where the deposition parameters were as follows: base pressure – 4×10^{-9} Torr, laser pulse rate of 5 to 10 Hz, laser radiation wavelength – 248 nm and pulse width 25-35nsec, laser pulse energy (exit port) of 600-800 mJ with energy density 3.0-4.0J/cm^2. For dc magnetron-sputtering deposition Ar gas of 99.999% purity was used at a flow rate of 20 sccm during deposition. A hollow cathode electron source was used to sustain the discharge at 4×10^{-2} Pa (Ar) during deposition. Ta films of 90 nm thickness were deposited at 300W, which yields a deposition rate of about 50 nm/min. The films were analyzed by X-ray diffraction using a Rigaku Diffractometer equipped with Cu-K$_\alpha$ source operating at a power as high as 5KW. The RBS (Rutherford backscattering) measurements using 2.0MeV α ions were made to estimate the oxygen content in the films. The nature of the microstructure in these films was studied using cross-section samples in a 200-keV JEOL 2010F high-resolution transmission electron microscope (HRTEM) with point-to-point resolution of 1.8

Å. These samples were annealed at a base pressure of 1×10^{-10} Torr up to 700 °C. SIMS, STEM-Z contrast imaging and EELS with 0.16nm resolution were used to study Cu diffusion behaviors in Ta films with different microstructures. SIMS analysis was performed using CAMECA IMS-6f. A 10 keV, 200nA Cs^+ primary ion beam was rastered over an area of 150x150 μm^2 with the mass resolution of 1600 m/Δm.

Fig. 2 shows the XRD pattern of the films deposited on Si (100) at room temperature by PLD, laser-MBE and DC magnetron sputtering. A sharp peak corresponding to polycrystalline β–Ta (002) is observed for the film deposited by sputtering, a relatively weaker peak corresponding to α-Ta (110) for the film deposited by laser-MBE and a broad peak is observed for the film deposited by PLD. The broad peak indicates that the film deposited by PLD is amorphous. To confirm the amorphous structure of the Ta film deposited by PLD, a high-resolution TEM study was performed. Fig. 3 (a) is a low magnification cross-section image of the Ta/Si (100) which shows that the film thickness is ~50nm. Fig. 3 (b) is a high resolution image of Ta/Si interface, where Ta film is seen to be amorphous and the structure of crystalline silicon substrate provides as a standard for the amorphous structure of the Ta film. The film structure is completely amorphous and no regions with any local ordering are observed. The selected area diffraction pattern (SAD) shown as an inset in fig. 3 (b) illustrates a diffused ring pattern, which is characteristic of the amorphous materials. The Ta/Si interface is fairly sharp and free of any visible oxide layer. Fig.4. is a SEM micrograph of the Ta film deposited by PLD showing the surface morphology. From the micrograph it can be observed that the film surface is smooth free of any observable defects such as voids or porosity. Another notable observation is that even at high magnification no grains could be revealed which

7 Narayan

also suggests that the film is amorphous. The EDS on the Ta film surface is shown as an inset in Fig.4 and it shows no indication for the presence of O or N in the film within its detection limit.

The oxygen content in the films was also investigated by EELS in high-resolution TEM and RBS (Rutherford backscattering) techniques. Fig. 5(a) is a high magnification TEM image showing the various locations in the Ta film including the Ta/Si interface at which the EELS was carried out and Fig. 5 (b) shows the corresponding EELS spectra. From the EELS spectra it can be observed that the concentration of O and N at the interface and in the interior film is considerably low and cannot be detected by EELS. Only element detected inside the film was Si ~ 1nm from the interface. The RBS and channeling confirmed the amorphous tantalum structure as there was no difference between the random and aligned channeling yields. The random spectrum showed some indication of oxygen scattering with an estimated concentration of less than 0.1%.

To form amorphous films, material is energized, e.g. by melting, dissolution, or irradiation and then de-energized rapidly by bringing dissimilar surfaces together and further de-energized to kinetically trap the amorphous form at a temperature that formation of crystalline phase is suppressed [10]. The mechanism of the formation of amorphous Ta during PLD is surmised to result from oxygen impurity, which reduces the mobility of Ta atoms on the substrate. The Ta atoms are effectively quenched into their sites when oxygen atoms reduce their mobility. This reduction in mobility prevents the development of any long-range ordering needed for recrystallization of Ta films. We can

generalize this mechanism by introducing relatively immobile impurities during deposition and it is possible to prevent the development of long-range ordering and render the structure amorphous. The α-Ta films were formed by pulsed laser deposition under an ultra high vaccum $<10^{-7}$ torr conditions where oxygen impurity content was extremely small. The films deposited at 25^0C under these conditions showed grain size of 10-20nm, and the grain size increased with substrate temperature and produced epitaxial films at 650^0C and higher. The epitaxial growth of α-Ta films was realized via domain matching epitaxy with TiN buffer layer where integral multiples (4/3) of lattice planes matched across the film-substrate interface[11].

Films deposited by the dc-magnetron sputtering were predominantly (002) oriented β-Ta phase as shown by the X-ray diffraction pattern in the figure 6(a). The HRTEM image of β-Ta film in the figure 6(b) along with the diffraction pattern in the insert shows the polycrystalline nature of the Ta film with the average grain size of around 30nm. Ta layer is predominantly oriented in the (002) direction with its lines fringes parallel to the interface. Selected area electron diffraction patterns of a cross-section samples shows a strong orientational relationship between Cu (111) and Ta (002) aligned with Si (001). The alignment of Cu (111) with tetragonal symmetric β-Ta atoms requires pseudohexagonal atomic arrangement in the (002) β-Ta plane for the heteroepitaxial growth with the misfit strain 7.6 % [12].

After attaining the amorphous and polycrystalline microstructures of Ta films, all the samples were annealed simultaneously at 650°C ± 30 °C for 1 Hr to compare the effect of microstructure on diffusion behavior of Cu. After annealing, the presence of undiffused Cu on Ta films could overshadow the signal from the diffused Cu in Ta films

for the SIMS experiment. To overcome this, the Cu films on top of Ta films were removed with an etching agent consisting of (NH_4OH (20ml); H_2O_2 (20 ml), H_2O (10ml)). SIMS profiles for Cu diffusion in amorphous Ta after annealing at $650^\circ C \pm 30^\circ C$ for 1 Hr is shown in the figure 7 (a) and compared with the unannealed samples as shown in the figure 7 (b). Amorphous films lack grain boundaries, which act as rapid diffusion paths to assist rapid diffusion and are more robust diffusion barrier. As seen in the figure 7, there is an insignificant change (within the sensitivity of SIMS $\leq$ 10nm) in the profile of Cu in the amorphous Ta film for both annealed and unannealed samples and also no Cu signal is observed inside the Si substrate, which points to insignificant diffusion of Cu into the amorphous Ta films. Presence of impurities like O rendering the amorphization of the Ta films by PLD and in diffusion of Si into the film can be seen in the SIMS profile for both annealed and un-annealed samples. Similarly, the SIMS profiles for the diffusion of Cu in polycrystalline Ta films for annealed and un-annealed samples are shown in the figure 8(a) and figure 8(b), respectively. The pseudocolumnar growth of polycrystalline films containing grain boundaries, which connect the overlayers with the substrate, serve as a fast diffusion paths for Cu. Significant diffusion of Cu in the annealed polycrystalline Ta films is observed as seen in the figures due to a significant increase in the Cu signal compared to the unannealed sample inside Ta films. Significant increase of Cu signal inside the Si substrate as compared to the unannealed samples also confirms the excessive diffusion of Cu in polycrystalline Ta films. The peaks in the SIMS profiles are observed due to the differences in the yield of Cu signal in Ta and Si matrices. Amorphous Ta films by PLD shows significantly less diffusion of Cu as compared to the polycrystalline Ta films.

Diffusion in the amorphous Ta film was also studied with Z-contrast imaging and EELS, which provide chemical composition and information on bonding characteristics [13]. Figure 9(a) shows the Z-Contrast image of Cu/Ta (PLD 650°C)/Si sample annealed at 650°C for 1 Hr where the probe formed by the electron beam was scanned across the Ta films to detect the Cu signal with EELS as shown in Fig. 9(b), where the Cu-L_3 edge onset corresponds to 931eV. The total diffusion length of the annealed amorphous sample is around 10nm. Similar diffusion studies done for the single crystal sodium chloride structure TaN films by similar STEM imaging technique showed similar diffusion length of ~10nm for the given temperature and time [14]. From a structural perspective, by comparing all TaN$_x$ phases, which can be simply described as close-packed arrangements of Ta atoms, with the smaller N atoms inserted into interstitial sites due to which the resulting structure has significantly higher resistance to Cu diffusion than does the pure Ta metal. However, amorphous Ta films by PLD due to lack of interstitial sites are as effective diffusion barriers as single crystal TaN films. Hence Ta films deposited by PLD can eliminate the issues of using different precursors and techniques to achieve stoichometric TaN and also the variations in the resistivity behavior of various TaN$_x$ phases [15] can be avoided.

The amorphous nature of the Ta film was found to be stable uptill 700°C above which the films starts to recrystallize as shown in the HRTEM image of annealed Ta film in the Figure 10. SIMS experiment at this temperature for both amorphous and polycrystalline Ta films showed significant diffusion of Cu in Ta film and Si substrate due to grain boundary diffusion. The single-crystal Ta films, on the other hand, were

Narayan

found to be extremely stable with temperatures over 800^0C and no significant diffusion of copper into single-crystal Ta films was observed.

To lower the RC delay in the integrated circuits for future generation devices barrier layers also play a significant role in governing the resistivity of interconnects. The microstructures of the barrier layers play an important role in the resistivity behavior of the films. Figure 11 shows the resistivity behavior in the temperature range of 12-300K of the amorphous film grown by PLD and of polycrystalline film grown by the MS. It is quite interesting to note that the amorphous films exhibit negative temperature coefficient of resistivity (TCR) values whereas polycrystalline films show positive TCR behavior. Similar transitions in the TCR behavior from negative to positive have been observed previously [16] which can be attributed to change in the crystal structure. The negative TCR behavior in amorphous film is due to the weak localization and enhanced electron-electron interaction in the system which have been observed in several other metals and alloys [17]. As compared to pure β-Ta with resistivity of ~220μΩcm [15], the resistivity values of amorphous Ta films produced by laser ablation is in the range of ~275 μΩcm at room temperature and decreases at higher temperature due to its negative TCR behavior to satisfy the constraints of the delays in interconnects. The room-temperature reistivity of α-Ta was determined to vary 15-30μΩcm as the microstructure changed from single-crystal to nanocrystalline materials.

In summary, the present invention claims to fabricate amorphous, nanocrystalline, polycrystalline and single-crystal Ta films by pulsed laser deposition and dc magnetron sputtering techniques. X-ray diffraction and high-resolution transmission electron

12 *Narayan*

microscopy techniques confirm the microstructure of these films. The formation of amorphous Ta is linked to trace amount of oxygen introduced during deposition. The oxygen atoms trap Ta atoms locally and prevent the structure from establishing a long-range order. Single-crystal Ta films on silicon were stable with temperature over 800^0C, while amorphous Ta films recrystallized at 700^0C and above. The resistivity measurements in the temperature range (10-300K) showed room-temperature values to be 15-30μ Ω-cm for α-Ta, 180-200μ Ω-cm for β-Ta and 250-275μ Ω-cm for a-Ta. The temperature coefficient of resistivity (TCR) for α-Ta and β-Ta were found to be positive with characteristic metallic behavior, while TCR for a-Ta was negative characteristic of high-resistivity disordered metals. The diffusion characteristics of Cu/Ta/Si layers showed amorphous Ta and single-crystal Ta to be a far superior diffusion barrier than polycrystalline Ta films where grain boundaries provided rapid diffusion paths for copper. However, amorphous structure lost its superior diffusion properties after recrystallization at 700^0C. Thus, single crystal and amorphous Ta films combined with low-resistivity of α-Ta provide an excellent solution for Cu diffusion problem in next-generation silicon microelectronic devices.

References

1.   J. O. Olowolafe, J.Li, J.W. Mayer: J. Appl. Physics. **68**(12), 6207 (1990).

2.   S.P. Murarka, Mater. Sci. Eng., R. **19**, 87 (1997).

3.   A. E. Kaloyeros and E. Eisenbraun, Annu. Rev. Mater. Sci. **30**,363 (2000).

4.   Massalski TB. 1990. *Binary Phase Diagram*. Westerville, OH: Am. Soc. Met.

5.   G. Ottaviani. *Thin Solid Films* **140** (1985), p. 3.

6.   T. Ichikawa, M. Takeyama, A. Noya, Jpn. J. Appl. Phys., Part 1 **35**, 1844 (1996).

7.   D. Yoon, K. Baik and S. Lee, *J. Vac. Sci. Technol. B.* **17**(1): 174–81(1999).

8.   M. Stavrev, D. Fischer, A. Preu, C. Wenzel, N. Mattern; 1997, *Microelectron. Eng.* 33:269–75.

9.   T. Laurila, K. Zeng, J. Molarius, I. Suni, J.K. Kivilahti, J. Appl. Phys., **88**, 3377, (2000).

10.   L. J. Chen, Mat. Sci. & Engg. R: Reports, **(29)** 5, Sept.2000 (115).

11.   J. Narayan et al. Appl. Phys. Lett. 61, 1290 (1992); US Patent # 5,406,123(4/11/1995); J. Narayan and B. C. Larson, J. Appl. Phys. 93, 278(2003).

12.   K. W. Kwon, C. Ryu, R. Sinclair, S. S. Wong, Appl. Phys. Lett. **71**, 3069 (1997).

13.   S. Lopatin, S. J. Pennycook, J. Narayan, and G. Duscher, Appl. Phys. Lett. **81** 2728 (2002).

14.   H. Wang, A. Tiwari, X. Zhang, A. Kvit, and J. Narayan J, Appl. Phys. Lett, **81** ,1453 (2002).

15.   H. Kim, A. J. Kellock, and S. M. Rossnagel, J. Appl. Phys., **92** (12), 7080 (2002).

16.   P. Catania, R. A. Roy, and J. J. Cuomo, J. Appl. Phys. **74** (2), 15 July (1993).

17.   M.A. Howson, D. Greig, Phys. Rev B, **30**, 4805,1984.

Brief Description of the Drawings

Figure. 1 Schematic cross-section view of formation Ta films **1110** on silicon substrate **1100** without buffer (Figure 1(a)) and with buffer layer **1120** (Figure 1(b)).

**Figure.2** XRD spectra of Ta films deposited on Si(100) substrate by pulsed laser deposition and magnetron sputtering.

Figure 3. <110>Cross-section TEM micrograph of Ta films on Si(100) substrate: (a) low magnification image showing the entire thickness of amorphous layer; (b) high-resolution image with an inset showing the selected-area diffraction pattern of the amorphous phase.

Figure 4. Scanning electron microscopy (SEM) micrograph of the Ta film surface with inset x-ray EDS(energy dispersive spectroscopy) spectrum.

Figure 5. (a) Cross-section TEM image of the Ta film with the locations of the EELS analysis; (b) EELS spectra corresponding to locations 1,2,3 and 4 in figure (a).

Figure. 6 (a) X-ray diffraction pattern of the polycrystalline β-Ta films with (002) orientation; (b) High-resolution TEM images for polycrystalline Ta film grown by MS. The inserts are magnified Cu/Ta interface with absence of amorphous Ta_2O_5 and the diffraction pattern of the film.

Figure. 7 SIMS profiles of Cu/amorphous Ta (PLD)/Si film (a) annealed at ~650°C for 1 Hr. and (b) as deposited sample. Insignificant diffusion of Cu was observed in the amorphous Ta film. Presence of O and Si was observed in Ta films rendering the amorphisation of Ta films by laser ablation.

Figure.8 SIMS profiles of Cu/polycrystalline Ta (MS)/Si film (a) annealed at ~650°C for 1 Hr. and (b) as deposited sample. Significant diffusion of Cu was observed in polycrystalline Ta film as well in the Si substrate.

15 *Narayan*

Figure 9. High-resolution TEM images for Ta film grown by PLD and annealed at 700°C

± 30°C for 30 min causing the crystallization of the Ta film.

Figure 10. (a) Z contrast image for the amorphous Ta films annealed at ~650°C for 1 Hr.

The total diffusion distance is indicated by the arrows. (b) EELS spectrum for showing

the presence and Cu and O in the Ta films.

Figure 11. Electrical resistivity measurements of amorphous Ta (PLD) and

polycrystalline Ta (MS), in the temperature range 12 to 300K.

What is claimed is

1. A method for fabricating α-Ta and β-Ta films in the form of amorphous, nanocrystalline (grain size 10-100nm), polycrystalline (>100nm) and single crystal.

2. Single crystal films may be grown on silicon substrate by domain matching epitaxy.

3. Single crystal and amorphous tantalum with no grain boundaries show excellent diffusion barrier properties for copper.

4. Electrical resistivity values ranged from 15 μ Ω-cm at room-temperature for single crystal α-Ta, to 180-200μ Ω-cm for β-Ta and 250-275μ Ω-cm for a-Ta.

5. A microelectronic structure comprising: a silicon substrate and α-Ta and/or β-Ta films having amorphous, nanocrystalline, polycrystalline, and single crystal microstructures with and without buffer layers.

17 *Narayan*

Figure. 1 Schematic cross-section view of formation Ta films **1110** on silicon substrate **1100** without buffer (Figure 1(a)) and with buffer layer **1120** (Figure 1(b)).(Narayan)
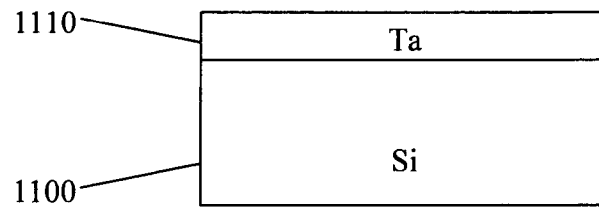
Fig. 1 (a)
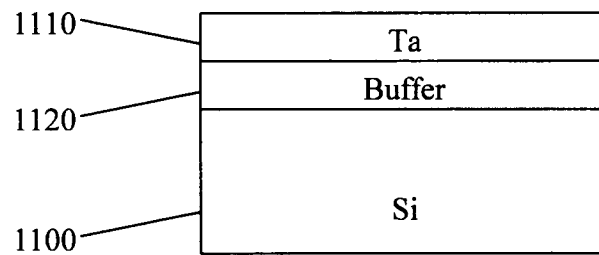
Fig. 1 (b)
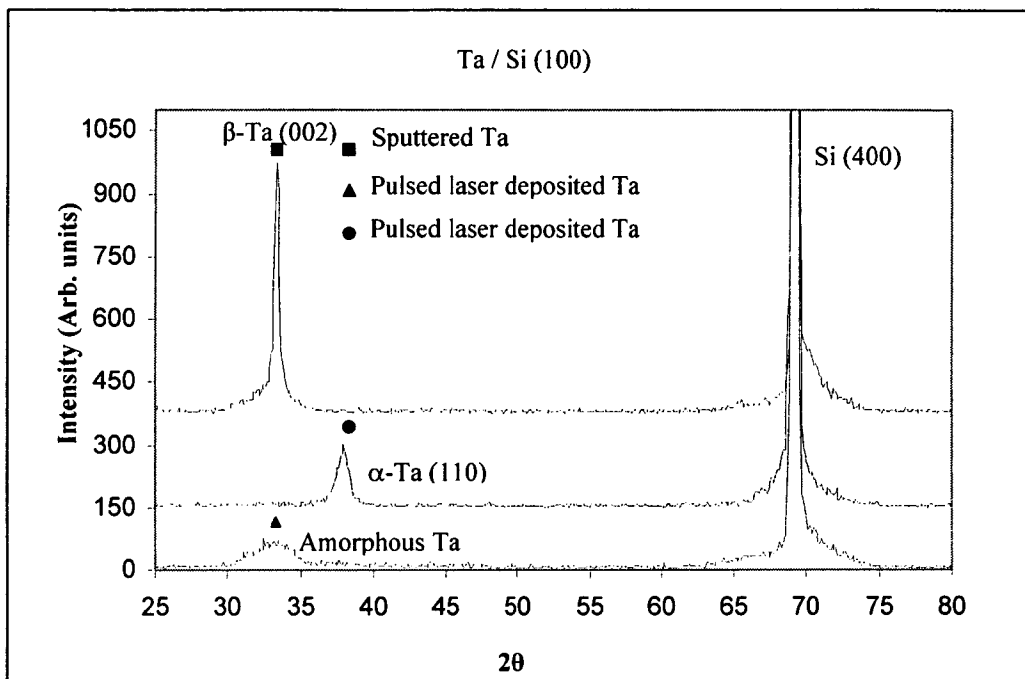
Fig. 2. Narayan
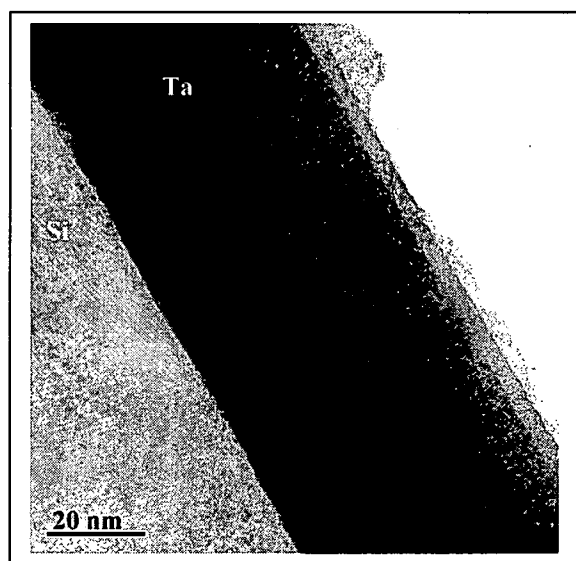
(a)
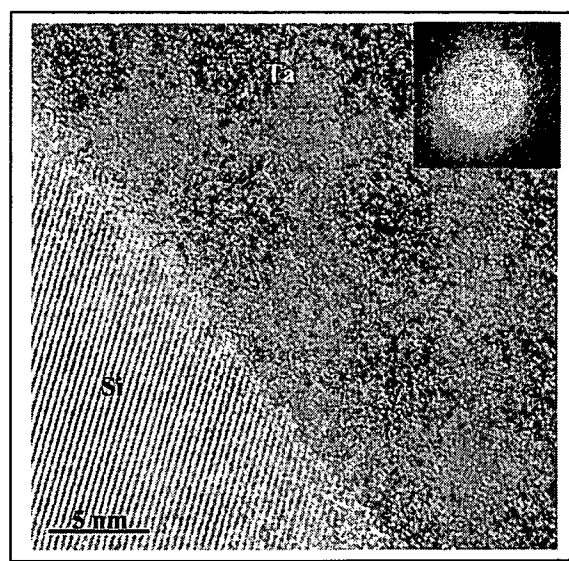
(b)

Fig. 3.Narayan.
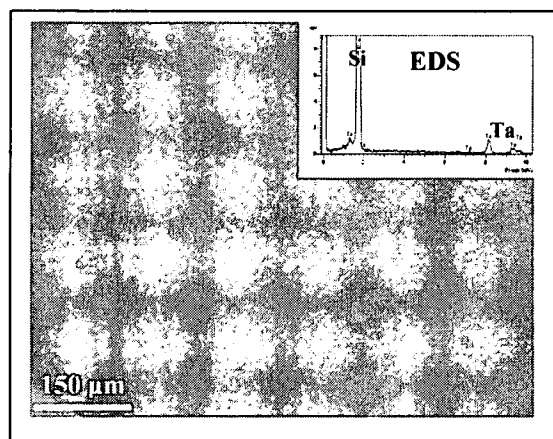
Fig. 4. Narayan
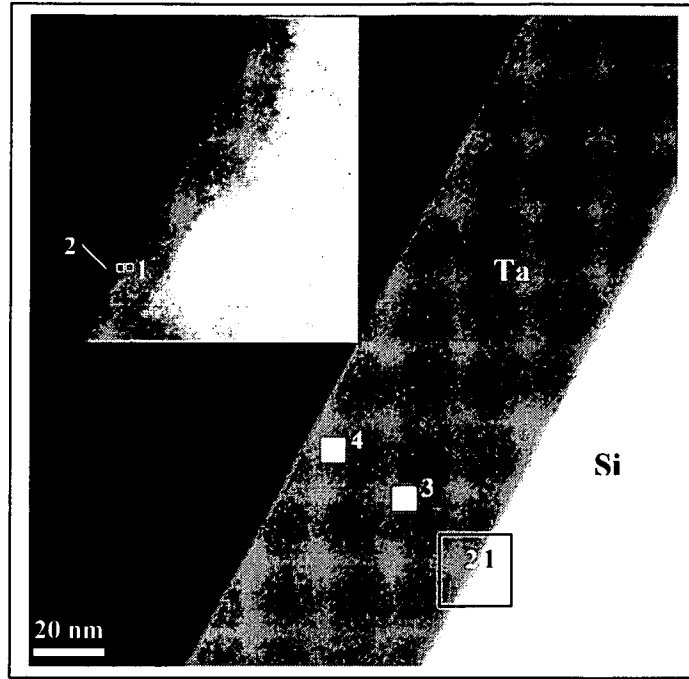
Fig. 5. (a) Narayan
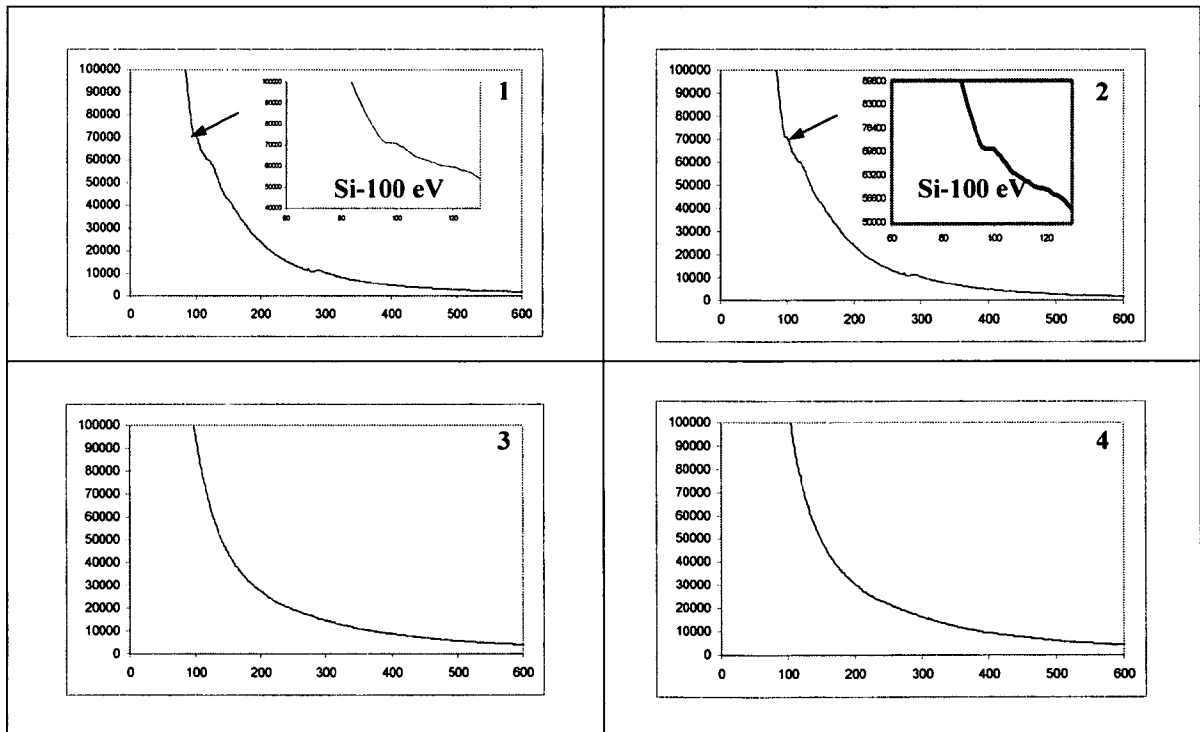
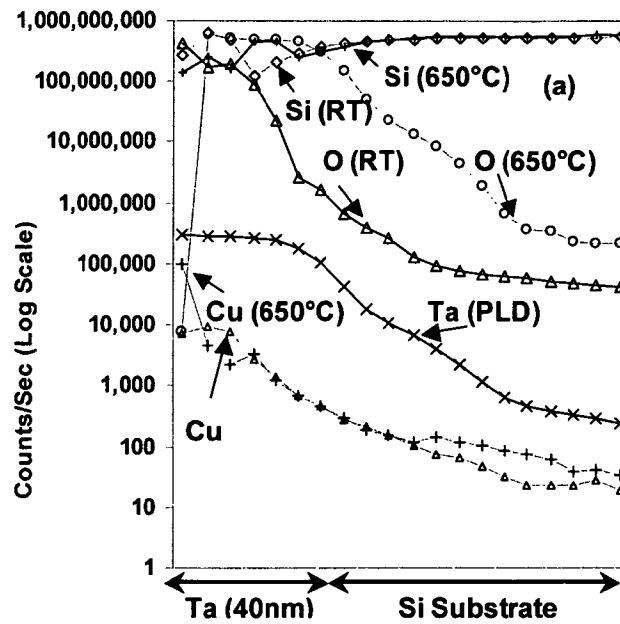Fig. 5 (b) Narayan
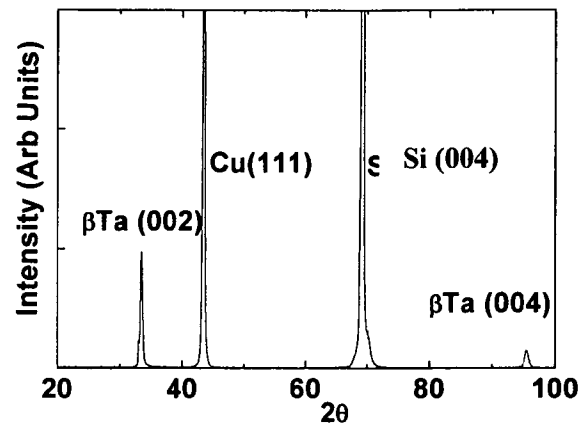
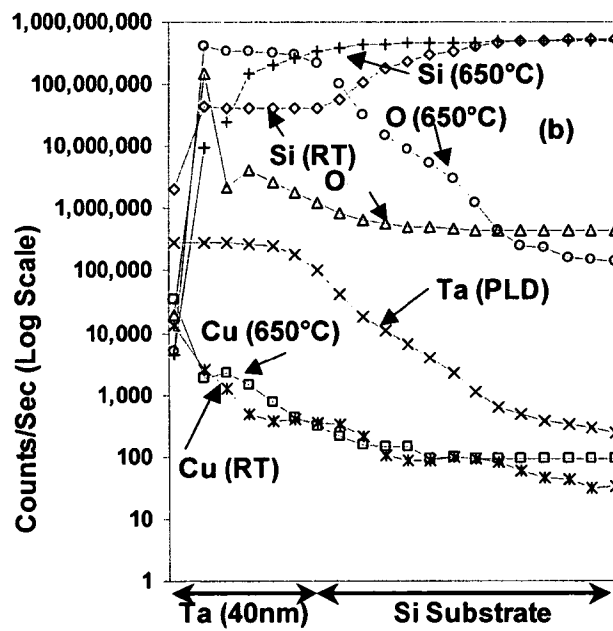Fig. 6. (a) Narayan
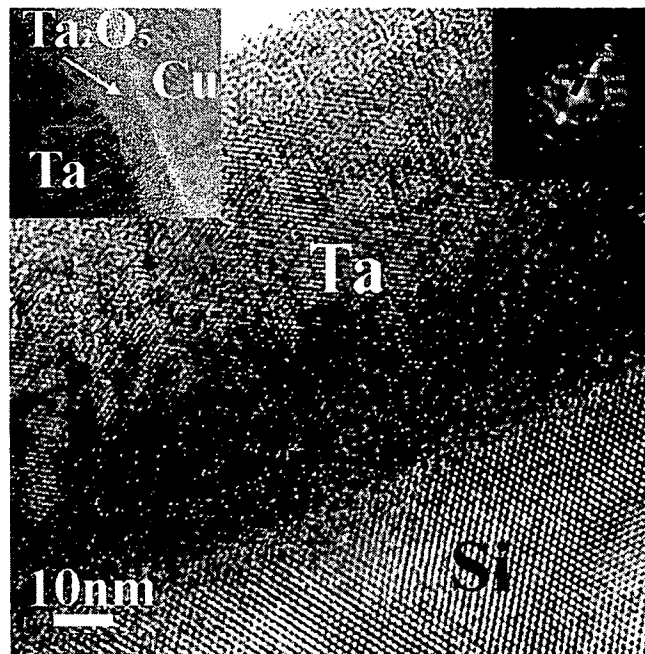
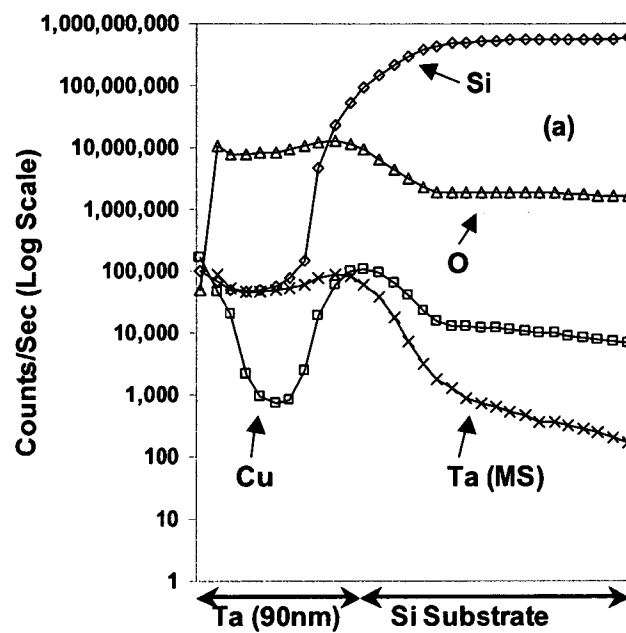Fig. 6. (b) Narayan

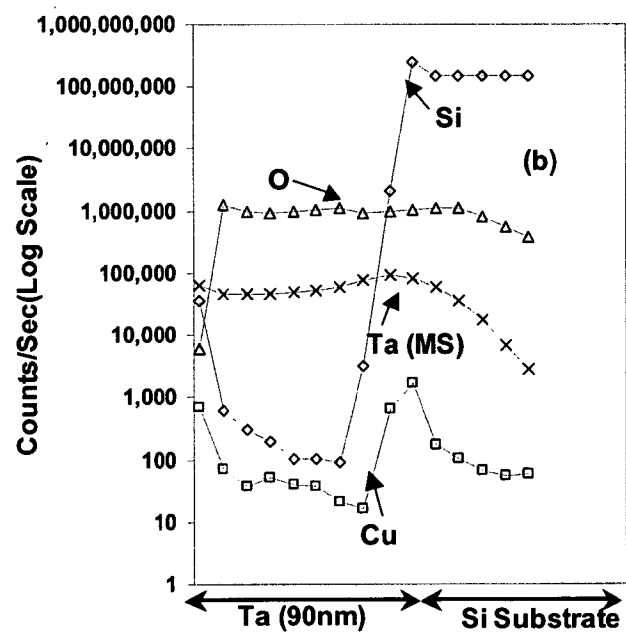Figure 7(a) Narayan

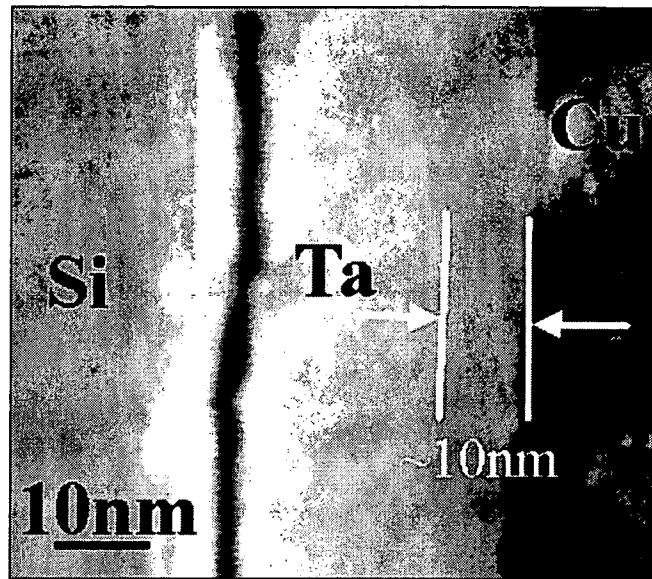Figure 7(b) Narayan

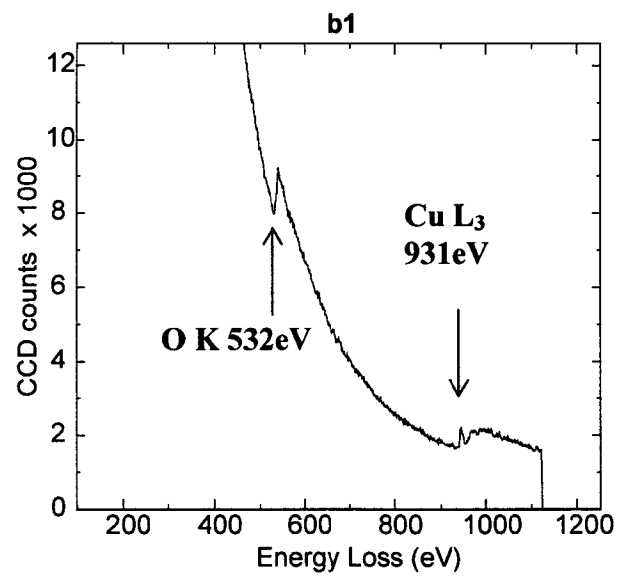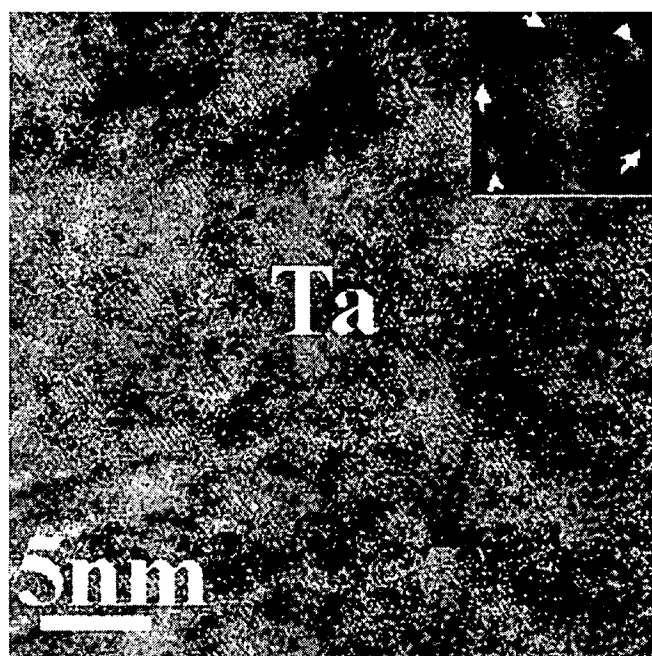Fig. 8. (a) Narayan

Fig. 8. (b) Narayan

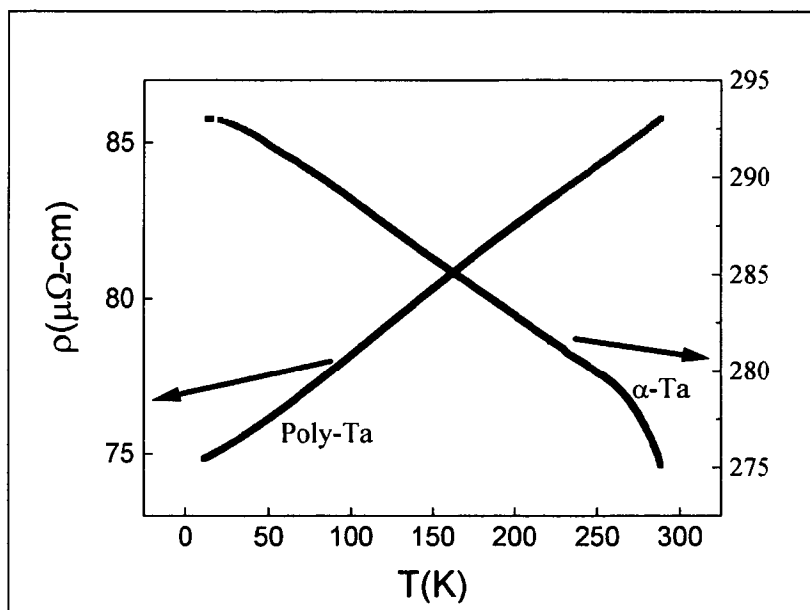Fig. 9(a). Narayan

Fig. 9. (b) Narayan

Fig. 10. Narayan

Fig. 11. Narayan